Behavioral/Systems/Cognitive

Neural Correlates of Context-Dependent Perceptual Enhancement in the Inferior Colliculus

Paul C. Nelson and Eric D. Young
Center for Hearing and Balance, Department of Biomedical Engineering, Johns Hopkins University, Baltimore, Maryland 21205

In certain situations, preceding auditory stimulation can actually result in heightened sensitivity to subsequent sounds. Many of these phenomena appear to be generated in the brain as reflections of central computations. One example is the robust perceptual enhancement (or "pop out") of a probe signal within a broadband sound whose onset time is delayed relative to the remainder of a mixture of tones. Here we show that the neural representation of such stimuli undergoes a dramatic transformation as the pathway is ascended, from an implicit and distributed peripheral code to explicitly facilitated single-neuron responses at the level of the inferior colliculus (IC) of two awake and passively listening female marmoset monkeys (*Callithrix jacchus*). Many key features of the IC responses directly parallel psychophysical measures of enhancement, including the dependence on the width of a spectral notch surrounding the probe, the overall level of the complex, and the duration of the preceding sound (referred to as the conditioner). Neural detection thresholds for the probe with and without the conditioner were also in qualitative agreement with analogous psychoacoustic measures. Response characteristics during the conditioners were predictive of the enhancement or suppression of the ensuing probe response: buildup responses were associated with enhancement, whereas adapting conditioner responses were more likely to result in suppression. These data can be primarily explained by a phenomenological computational model using dynamic (adapting) inhibition as a necessary ingredient in the generation of neural enhancement.

Introduction

Sound perception is context dependent, often to an extent that is difficult to reconcile with peripheral neural responses. In the frequency domain, for example, simultaneously presented stimulus components can either impair (Yost and Sheft, 1989) or enhance (Hall et al., 1984) performance in detection tasks at frequency separations that likely result in little or no interaction between the target and masker in auditory nerve (AN) fibers. In the temporal domain, listeners' performance (Jesteadt et al., 1982) tends to be much more strongly affected by the presence of a preceding (forward) masker than AN fiber responses in a similar paradigm (Relkin and Turner, 1988). How these and other psychophysical phenomena are influenced by central auditory processing remains an open question.

The purpose of this study was to investigate the neural basis of a robust perceptual phenomenon that exemplifies context dependence across the dimensions of both frequency and time. When the onset of a tone is delayed with respect to the remainder of a longer broadband signal (referred to as the conditioner), the delayed signal stands out clearly as a tonal sensation (Hartmann and Goupell, 2006), separate from the rest of the stimulus. If the onset times are matched, the tonal percept disappears and a single object is heard whose specific characteristics are determined by the frequency content of the conditioner and probe mixture. Many psychoacoustic findings reflect this type of effective enhancement or "pop-out." For example, detection thresholds for the introduced component are lower (better) when its onset is delayed (Viemeister, 1980; Carlyon et al., 1989; Wright et al., 1993), and the delayed component acts as a more effective forward masker of a subsequent probe sound (Viemeister and Bacon, 1982; Thibodeau, 1991; Wright et al., 1993). It is the robust nature of the phenomena demonstrated in these psychoacoustic studies (notably using quite different stimuli and parameter spaces) that suggests that many spectrotemporally complex natural sounds are also likely to engage the mechanisms underlying enhancement.

In apparent contrast to the enhanced percept of the introduced tone, single AN fibers actually respond less when the probe tone is delayed than when its onset is shared with the remainder of the mixture (Palmer et al., 1995). To explain the percept with peripheral responses, a population of AN fibers with different frequency tuning properties must be considered. Fibers with best frequencies (BFs) close to the frequency of the enhanced tone exhibit less suppression of their response given the conditioning stimulus than fibers with further removed BFs (Palmer et al., 1995). Therefore, the peripheral neural code for auditory enhancement is distributed and implicit.

Here, we show that, at the level of the inferior colliculus (IC) in awake and passively listening marmoset monkeys, many single neurons exhibit strongly facilitated responses to delayed-onset BF tones. Such an explicit and direct correlate for enhancement has not been reported previously at any level of the auditory

Received Jan. 18, 2010; revised March 18, 2010; accepted March 26, 2010.

This study was supported by National Institutes of Health Grants DC00115 and DC009164. We are grateful to Sean Slee, Bradford May, and two reviewers for comments on previous versions of this work and to Xiaoqin Wang, Yi Zhou, Jenny Estes, and William Tam for help with animal preparation and care.

Correspondence should be addressed to Paul C. Nelson, 505 Traylor Research Building, 720 Rutland Avenue, Baltimore, MD 21205. E-mail: pcnelson@jhu.edu.

DOI:10.1523/JNEUROSCI.0277-10.2010

 0270-6474/10/306577-11$15.00/0

system. A relatively simple model of interactions between broadly tuned adapting inhibition and sharp excitation captures many of the critical features of the neural phenomenon.

Materials and Methods

The animal preparation, recording methods, and acoustic stimulus presentation have been described in detail previously (Nelson et al., 2009) and were based on previous studies in the awake marmoset auditory cortex (Lu et al., 2001). Briefly, animals were gradually adapted to sitting in a custom-made primate chair for several weeks before a sterile, isoflurane-anesthetized surgery was performed to mount posts for subsequent head fixation. After a recovery period of ~2 weeks, a small (~1 mm diameter) craniotomy was made to provide access to the IC using a lateral-access approach. Multiple craniotomies were made in each animal, and the preparation allowed for daily recording sessions for well over 1 year per animal. The marmosets sat in a comfortable seated position with their heads held in a natural orientation facing a speaker (FT-28D; Fostex) positioned ~1 m directly in front of them. An epoxy-coated tungsten microelectrode (A-M Systems) was advanced with a hydraulic microdrive through the dura and through up to 1 cm of brain tissue before reaching the IC. All procedures were approved by the Johns Hopkins University Institutional Animal Care and Use Committee and conformed to National Institutes of Health standards.

Spike times of well isolated single-unit extracellular neural responses were recorded in the physiologically identified central nucleus of the inferior colliculus (CNIC) in two awake and passively listening adult female marmoset monkeys (*Callithrix jacchus*). We assumed that neurons were located in the CNIC based on a well defined location within the tonotopically organized frequency laminae along with reliable, nonhabituating, and short-latency (less than ~20 ms) auditory responses.

Before presenting the enhancement paradigm stimuli, each neuron was characterized with a response map [200 ms pure tones presented (1/s) over a wide range of frequencies and levels] and a rate-level function for BF tones. Enhancement and suppression were identified by comparing responses to a "test" stimulus with and without a preceding "conditioner." To form the test stimulus, a BF probe tone was presented simultaneously with flanking bands of multiple tones. The flanking bands also formed the conditioning stimulus that was presented before the introduction of the BF tone. The conditioner (C) was 500 ms in duration (unless this parameter was explicitly varied) (see Fig. 4), with 10 ms raised-cosine rise and fall ramps, and was composed of equal-amplitude, logarithmically spaced (1/10 octave spacing) random-phase tonal components, spanning a range from 200 Hz to 25.6 kHz. The choice of logarithmic (rather than harmonic) frequency spacing results in a qualitatively noise-like percept, without a fundamental frequency or clear pitch. A spectral notch (SN) was carved out of the C spectrum surrounding the BF of each neuron by removing the components within a given range (from 0–2 octaves). The 100 ms test complex (10 ms rise/fall) was presented either in isolation [test-alone (T)] or immediately after the conditioner [conditioner-then-test (CT)]. The test complex had a spectrum identical to that of the conditioner, except for the addition of a component at the BF of the neuron. At least 600 ms of silence separated the T offset and C onset between stimulus presentations, and the three arrangements (T, C, and CT) were presented in an interleaved manner for each parameter value (e.g., SN width) before continuing on to the second repetition of the various conditions. All stimuli were repeated 10 times.

Overall sound level was also varied when time allowed, using three fixed sound pressure levels (SPLs): 20, 40, and 60 dB above the threshold of the most sensitive neurons for an individual (BF) component (~0 dB SPL). These values are approximately the level per component in decibels SPL, and therefore the overall SPL in the no-notch condition ranged from 38 to 78 dB. The data in Figure 3 were generated by presenting either the low-frequency (below BF) or high-frequency (above BF) portions of the C before the T complex, which included both the low- and high-frequency sides of the spectrum. In Figure 4, the duration of the conditioner was varied from 32 to 512 ms (five log-spaced durations). Finally, to estimate neural detection thresholds (see Fig. 6), the level of the BF component was varied independently of the remainder of the T complex, over a range from 20 dB below to 10 dB above the SPLs of the other components.

Spike-rate distributions were quantified using a discriminability index: $D = (R_{CT} - R_T)/[(\sigma_{CT} + \sigma_T)/2]$, where R_{CT} and R_T represent test-complex average spike rates, and σ_{CT} and σ_T are corresponding across-repetition SDs in the CT and T conditions, respectively (Simpson and Fitter, 1973). Firing rate during the test complex was measured over a 100 ms interval delayed by 8 ms with respect to the test sound onset at the speaker; this delay is based on the minimum observed response latency of the sample of CNIC neurons. As a rough descriptor of the temporal evolution of the response to the condition, a buildup to adaptation ratio (see Fig. 5) was defined as the average spike count in the initial 100 ms of the C response divided by the average count in the final 100 ms of the C response (the counting windows were again delayed by 8 ms with respect to sound onset). Values less than one indicate a buildup pattern in the response to the conditioner, whereas values greater than one are obtained when the response profile adapts (decreases) over time.

A computational model was developed to provide some insight into possible mechanisms underlying enhancement and suppression. The specific implementation of the model used responses from a previously described AN model (Heinz et al., 2001) as inputs to the putative central processing mechanism. All inputs were from the human "linear sharp" version of the Heinz et al. (2001) AN model with an assumed spontaneous rate of 50 spikes/s. Similar results were obtained with nonlinear (level-dependent) versions of the model, both with and without suppression (i.e., models 1 and 2 in the study by Heinz et al., 2001).

Two paths were assumed to converge on a central neuron: an excitatory channel tuned to the probe tone frequency (i.e., the model BF, 4 kHz for the example in Fig. 7) and an inhibitory channel whose response was defined as the sum of 16 model AN fibers logarithmically spaced with BFs ranging from 2 to 5.66 kHz (1 octave below to 0.5 octaves above the excitatory BF). The relative strength of the inhibitory inputs dropped off with distance from BF, using a triangular weighting function (on log-frequency axes) with its peak matched to the excitatory BF. The inhibitory response was smoothed (by convolution with an α function, $\tau = 2$ ms) and delayed by 1 ms before being subtracted from a smoothed ($\tau = 0.5$ ms) version of the excitatory channel. The model was robust to perturbations in the choices of smoothing and delaying parameters for these stimuli, which have relatively slow time courses. Finally, the difference between excitation and inhibition was half-wave rectified to eliminate negative firing rates.

The overall strength of the inhibitory input to the model was a critical parameter that was systematically varied (see Fig. 7). Only a single stage of inhibition was modeled (in contrast to Nelson and Carney 2004, 2007) and can be considered to represent net inhibitory effects accumulated along the pathway. It was necessary to assume some variability in the model responses to estimate discriminability (D values) comparable with the data. To do this, we fit a second-order polynomial to the SD versus average rate function from our actual IC data (supplemental Fig. S3, available at www.jneurosci.org as supplemental material). All simulations and data analyses were performed in MATLAB.

Results

IC neurons exhibit both enhancement and suppression

Responses of neurons in the CNIC were recorded in awake marmosets to the stimuli schematized at the top of Figure 1. A BF probe tone (100 ms duration) was accompanied by flanking bands of multiple logarithmically spaced tones (0.1 octave spacing, extending from 0.2 to 25.6 kHz). The BF probe tone was separated spectrally from the flanking bands by a notch width (NW) between 0 and 2 octaves. The flanking bands also formed a 500 ms "conditioning" stimulus presented before the introduction of the BF tone. The presence of the conditioning stimulus could either facilitate or suppress the spiking response to the test stimulus. Responses from four example neurons are illustrated in Figure 1*A–D* for a range of conditioner NWs. Note that the frequency spectra of the test stimuli were the same as the condi-

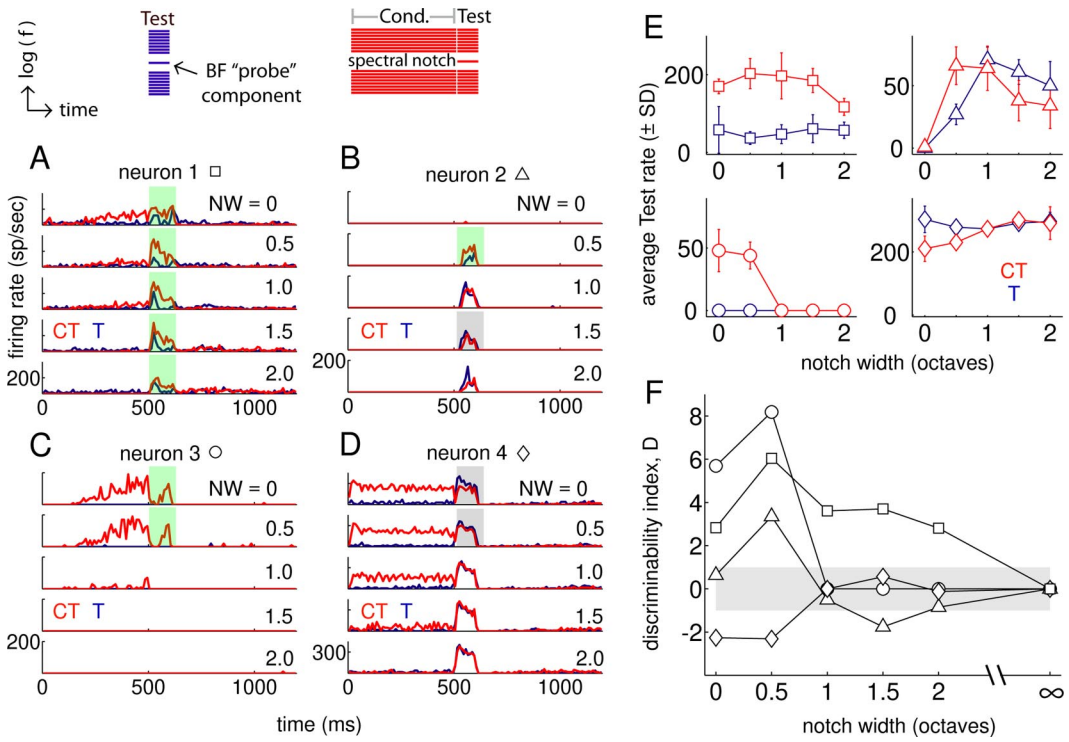

Figure 1. Example single-neuron responses to enhancement stimuli. ***A–D***, PSTHs (10 ms bins) of responses of four neurons to T (blue) and CT (red) stimuli over a 2 octave range of spectral NWs. Significantly enhanced (suppressed) responses are highlighted by the green (gray) squares. Stimuli are depicted as schematic spectrograms above ***A*** and ***B***. ***E***, Average ± SD firing rates measured in the 100 ms test-response window elicited by CT and T stimuli for the same four neurons and stimulus conditions as in ***A–D***. ***F***, Difference in the mean rates between CT and T responses normalized by the average across-repetition SD of the rate estimate, computed from the data shown in ***E***. The gray shading in ***F*** shows the $|D| < 1$ region.

tioner, except for the presence of the BF probe (at the same amplitude as the flanking tones). Responses to (physically identical) test stimuli (BF plus flanking bands) were compared with and without a preceding conditioner.

Peristimulus time histograms (PSTHs) are shown in Figure 1*A–D* for T (blue) and CT (red) stimuli over a 2 octave range of NWs. Conditioners could elicit a buildup response (Fig. 1*A*,*C*), an adapting response (Fig. 1*D*), or no spiking response (Fig. 1*B*). The conditioner presence could enhance (green shaded regions), suppress (gray shaded regions), or have no effect on (no shading) test responses. The strongest differences between the test responses in CT and T conditions tended to occur using narrower NWs (0 and 0.5 octaves), although neuron 1 exhibited enhanced test responses even with a spectral notch spanning 2 octaves.

Average ± SD firing rates in the 100 ms test-response epoch are shown in Figure 1*E* for the same four neurons, with (red) and without (blue) the preceding conditioner. These quantities (mean and across-repetition SD of the rate estimate) were used to establish the amount of enhancement or suppression in the form of a discriminability index *D*, defined as the difference in average rates (CT − T) normalized by the average SD of the two distributions (Fig. 1*F*). If the two distributions are approximately normal and have similar variances, this statistic is the well known d' measure of discriminability (Green and Swets, 1966). Positive (negative) *D* values indicate enhancement (suppression) of the test response, and absolute values greater than one are considered significant.

Several features emerge when the responses of the sample of 101 neurons are summarized with the *D* index. The majority of responses were affected by the presence of the conditioner for NWs ≤1.5 octaves, and, for nonzero NWs, the effect was predominately in the form of enhancement (Fig. 2*A*). The proportion of neurons with responses that were significantly modulated by the conditioner steadily decreased as the NW increased from 0.5 to 2 octaves. This falloff makes intuitive sense because, in the extreme of an infinitely wide notch, the comparison between CT and T responses would simply be between two BF tones with no preceding sound, resulting in identical responses and a *D* of 0. In the no-notch condition, test-response suppression was observed more often than enhancement, and more responses were unaffected by the presence of the conditioner than in the 0.5 octave case (Fig. 2*A*, open bars). These trends are consistent with on-BF forward suppression interacting with the mechanisms that generate enhancement away from BF (see below, Phenomenological model).

On average, the *D* statistic was a non-monotonic function of stimulus NW, with suppression dominating in the no-notch condition and enhancement reaching its maximum value at the narrowest tested NW of 0.5 octaves (Fig. 2*B*). The difference signal (DS) between the average PSTHs in the CT and T conditions (Fig. 2*B*, PSTH insets) show corresponding changes with NW. The initial 500 ms portion of the DS (preceding the red regions) shows the response to the conditioner, with excitation at narrow NWs and inhibition at broader NWs. Red regions in the DS plots show the response to the 100 ms test stimulus, which is negative for the 0 octave case reflecting suppression elicited by the conditioner. In contrast, the test-response DS for NW >0 is positive, indicating an enhanced test response. The magnitude of the enhancement declines over time (especially for larger NWs) but is still clearly present at the end of the 100 ms test signal.

Effects of other stimulus parameters on enhancement and suppression

Psychophysical studies have shown that perceptual enhancement depends on many stimulus parameters in addition to notch width. Here we show that the effects of overall sound level, con-

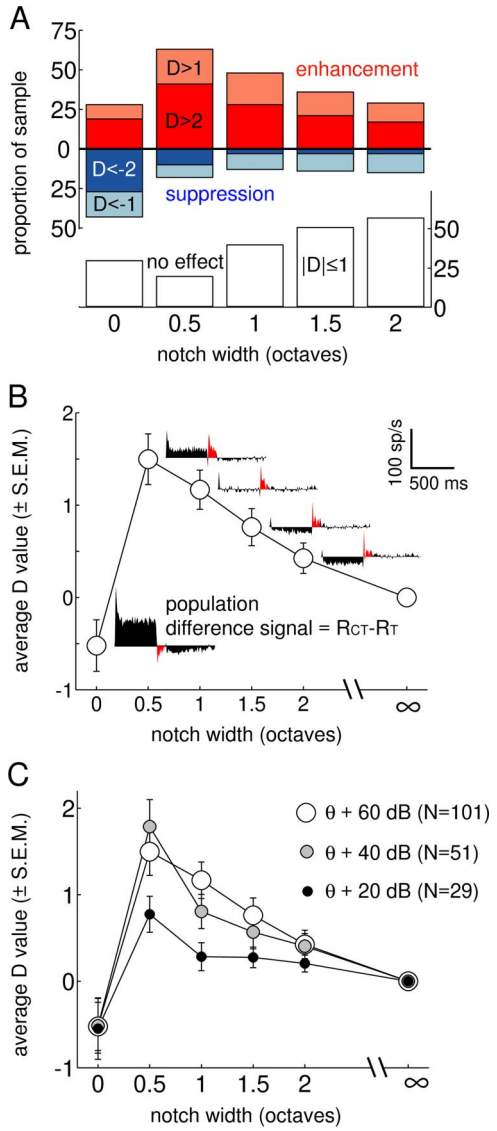

Figure 2. Summary of conditioner effects on responses to the test complex. ***A***, Proportion of neurons ($n = 101$) exhibiting enhanced ($D > 1, D > 2$) and suppressed ($D < -1, D < -2$) test responses as a function of conditioner NW. The remaining responses, unaffected by the conditioner ($-1 \leq D \leq 1$), are shown in the bottom bar graph (open bars). ***B***, Average ± SEM values of the *D* statistic over the 2 octave range of NWs tested. The cumulative DS for each condition are shown to the right of the points; red regions highlight the temporal position of the 100 ms analysis window for computing *D*. Scale bar corresponds to DS functions. ***C***, Effect of varying overall SPL on the NW dependence of the sample.

ditioner spectrum, and conditioner duration on responses of marmoset IC neurons, although diverse, are also broadly consistent with observations made in human psychoacoustics.

Robust, saturating level dependence

At low sound levels in human listeners, increasing the overall stimulus level often leads to an increase in the amount of enhancement observed, whereas at higher levels, the effect remains robust but tends to saturate (Viemeister, 1980; Strickland, 2004). The data presented above were all in response to a fixed and relatively high stimulus level: each tone component was ~60 dB above the thresholds of the most sensitive neurons at BF. This level will be referred to as 60 dB sensation level (SL); two other overall levels (20 and 40 dB SL) were also tested in a subset of the neurons. Average *D* versus NW functions for the three tested levels are shown in Figure 2*C*. The low-level (20 dB SL) stimulus resulted in less enhancement than the two higher-level stimuli, regardless of the NW. Medium- and high- level (40 and 60 dB SL) stimuli yielded similar patterns of enhancement and suppression in the sample average. This is consistent with the robust but saturating nature of the psychophysical phenomenon. Somewhat surprisingly, the no-notch condition resulted in nearly identical negative average *D* values for all three stimulus SLs (Fig. 2*C*, leftmost points). In other words, it appears that neural forward masking using these broadband masker and probe stimuli did not increase appreciably with level, as it does in other situations (Nelson et al., 2009).

Low-frequency components contribute more to response modulation

Perceptual enhancement can be generated with either low-pass or high-pass conditioners, as well as with the band-reject stimulus considered so far. When one side is presented in isolation, the low-frequency components produce more test–stimulus enhancement than the high-frequency components alone (Carlyon et al., 1989). To test whether IC neurons exhibit similar behavior, we compared responses to the test sound with either the low- or high-frequency portions of the conditioner presented alone or together (Fig. 3). The stimuli are shown at the top of Figure 3; note that the test–stimulus complex was identical in all three conditions (including both high- and low-frequency components along with the BF probe tone).

Data from four neurons are shown (Fig. 3*A*) to illustrate the heterogeneity of IC responses to this stimulus manipulation. Three of the four neurons exhibited enhancement with the complete stimulus (neurons 1, 2, and 4, left column), and neuron 3 was suppressed. However, only neurons 1 and 2 showed enhancement for the low-frequency conditioner (column 2), and only neurons 2 and 4 showed enhancement for the high-frequency conditioner (column 3). In the other cases, the neurons either showed suppression or no effect of the conditioner.

To summarize these diverse patterns, we compared *D* statistics derived from each stimulus configuration, reasoning that there should be a high correlation across the sample of cells between the *D* measured using the full stimulus and that observed using the portion of the conditioner that drives most of the overall enhancement or suppression. The low-frequency conditioner *D* values were reasonably correlated with the full-stimulus *D* values ($R^2 = 0.55$) (Fig. 3*B*, middle), although the relationship between the high-frequency conditioner *D* values and the overall *D* was weaker ($R^2 = 0.32$) (Fig. 3*B*, right). When contributions from the high- and low-frequency sides were combined by adding their respective *D* values, overall *D* values were predicted quite well ($R^2 = 0.73$) (Fig. 3*B*, left). Therefore, both low- and high-frequency conditioners could generate enhancement or suppression, but the low-frequency side drove more of the overall effect. This is qualitatively consistent with both the psychophysical data and the asymmetry of auditory tuning curves at levels up to the IC, with responses spreading further toward low frequencies than high (Kiang et al., 1965; Ramachandran et al., 1999). The magnitude of enhancement and suppression did not depend strongly on the BF of the neuron (*D* vs BF, $R^2 = 0.0014$) (supplemental Fig. S1, available at www.jneurosci.org as supplemental material), although the extent of the flanking band that is within the response area of the neuron is likely to differ at low and high BFs as a result of the limited range of the conditioning stimulus components (0.2–25.6 kHz). This result suggests the possibility that strong conditioner effects could probably be obtained

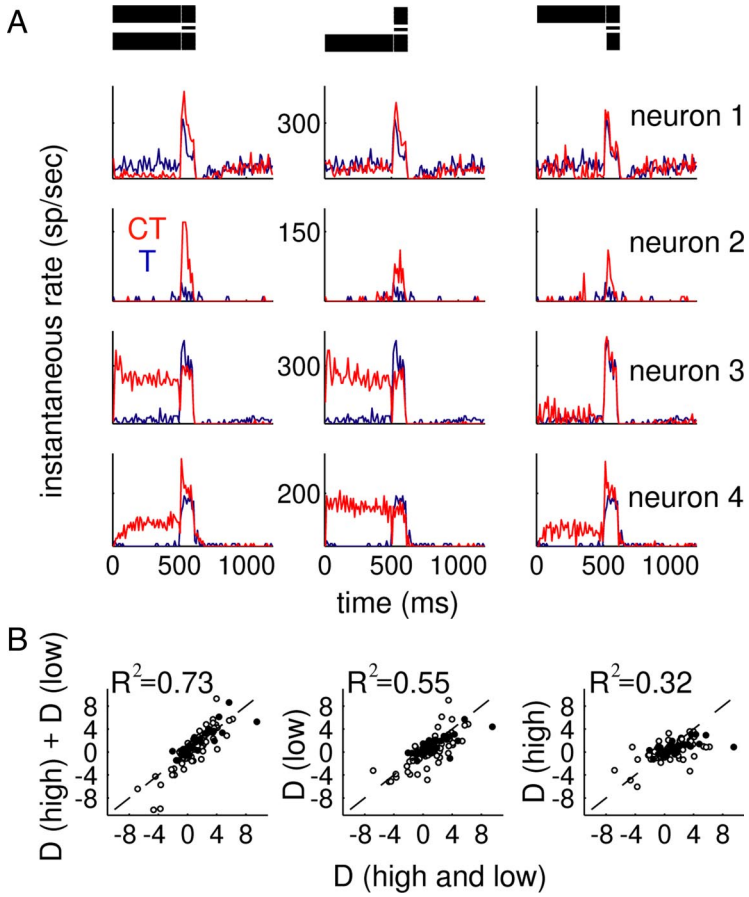

Figure 3. Below-BF energy in the conditioner drives more enhancement and suppression than above-BF components. ***A***, Single-neuron examples of CT (red) and T (blue) responses for four cells also tested with the above- and below-BF conditioner components presented in isolation. Neurons 1 and 2 were tested using a 1 octave notch; neurons 3 and 4 were tested with a 1/2 octave notch. Ordinate value ranges are fixed for each neuron (labeled in the middle panels); T responses are identical across the three columns. ***B***, Scatter plots of *D* values computed from isolated above- or below-BF conditioner components as a function of *D* values observed when the high- and low-frequency sides were presented simultaneously (abscissa). Two different NWs were used: 1/2 octave (open circles; $n = 71$) and 1 octave (filled circles; $n = 32$). Most neurons were tested with a 60 dB SL stimulus ($n = 70$); subsets of responses using lower-level sounds (40 dB SL, $n = 21$; 20 dB SL, $n = 12$) are also included.

using a stimulus with just a few components, a prediction consistent with the behavioral phenomenon (Viemeister, 1980).

Enhancement and suppression buildup over time

Enhancement effects in psychophysics are stronger when a longer conditioning stimulus is used (Thibodeau, 1991; Wright et al., 1993). Although the exact time course can be quite variable across listeners, it appears that a relatively slow process (on the order of several hundred milliseconds) produces enhancement in human listeners. Here, the time course of conditioner effects on test responses in IC neurons was investigated by varying the duration of the conditioner over a range from 32 to 512 ms. The test stimulus duration was always fixed at 100 ms.

The subgroup of neurons studied with various conditioner durations included test responses that were suppressed ($D < 1$; $n = 10$), enhanced ($D > 1$; $n = 23$), and unaffected ($|D| \leq 1$; $n = 19$) by the presentation of the longest conditioner (512 ms). Three neurons are represented in Figure 4*A* with PSTHs spanning the 300 ms window that includes the test responses in the CT and T configurations. The test response of neuron 1 was suppressed given the presence of the conditioner; the magnitude of this suppression increased over the range of durations tested. The (adapting) response to the conditioner can be seen in the panels with the shorter conditioner durations; by 512 ms after onset, this response was negligible (Fig. 4*A*, rightmost panel of neuron 1). The other two example neurons did not respond to the conditioner with spikes but did exhibit robust enhancement of the test response; the magnitude of the enhancement increased monotonically with conditioner duration in neuron 2 but seemed to saturate beyond 128 ms in neuron 3. Also, the enhancement was limited to the initial onset response in neuron 3 but persisted for the entire 100 ms test-complex duration in neuron 2.

Responses were grouped according to the *D* value measured with a 512 ms conditioner (Fig. 4*B*). Suppression and enhancement both tended to increase monotonically over the range of durations tested (left and right columns), and neurons that showed no effect at 512 ms did not show strong conditioner dependence at shorter durations (middle column). A 32 ms conditioning stimulus (Fig. 4*B*, leftmost points) was almost always insufficient to generate either enhancement or suppression. The duration effect for a typical neuron was reasonably well described by a straight line (on log-time coordinates) between $D = 0$ at 32 ms to the final *D* value of the function 512 ms. The fact that many functions did not appear to saturate or turn over (even between 256 and 512 ms) suggests the presence of a slow cumulative mechanism and may provide a neural substrate for the psychophysical effects observed at long conditioner durations.

Relationship to conditioner responses

As a first step in determining potential mechanisms underlying robust context-dependent enhancement and suppression, we considered the nature of the response to the conditioner itself and its relation to test-response modulation. One (essentially untested) model for the generation of enhancement includes inhibitory inputs that adapt over time (Viemeister and Bacon, 1982). Although inhibition cannot be directly observed in extracellular spiking responses, it seemed reasonable to assume that the responses of some neurons may allow for inferences about the feasibility of this model. If the putative inhibitory channels are adapting inputs from off-BF frequency regions and the conditioner effectively engages these inputs, then one might expect to see an increasing ("buildup") response to the conditioner alone in neurons that exhibit enhancement of a subsequent test complex.

To test this idea, the temporal evolution of conditioner-alone responses was generally quantified by taking the ratio of the average firing rate in the initial 100 ms of the response (C_i) to that in the final 100 ms of the response (C_f). This quantity (C_i/C_f) will be referred to as the buildup to adaptation (BU/A) ratio. Values less than one indicate buildup; values greater than one occur when the conditioner response decreases over time (i.e., adapts). Three representative PSTHs, along with the positions of the initial and

final windows (gray boxes), are shown above Figure 5*A*. These examples yielded BU/A ratios <1 (left), ~1 (middle), and >1 (right).

The relationship between *D* and the BU/A ratio is shown in Figure 5*A*. One feature that immediately stands out is the paucity of points in the bottom left quadrant, indicating that conditioners eliciting a strong buildup response were rarely associated with suppression. Instead, BU/A ratios less than unity were associated with positive values of *D* (or enhancement). This is consistent with the adaptation-of-inhibition hypothesis (although not strictly necessary for the model to be valid). When the response to the conditioner adapted (BU/A ratio >1), subsequent test responses could be either enhanced or suppressed, but the overall bias was toward suppression (the average *D* for BU/A ratios >1 was −0.37). The BU/A ratio was undefined when no spikes were observed during the C_f interval, and the ratio could not be plotted on the logarithmic axis in Figure 5*A* when no spikes were observed during the C_i interval. The proportions of these cases are shown in the bar graph inset in Figure 5*A*.

The same data are replotted in Figure 5*B* as histograms of the *D* statistic in each subgroup of conditioner response types. Adapting (blue histogram) and buildup (red histogram) conditioner responses occurred with nearly identical frequency (371 and 374 observations, respectively). The means (medians) of the two distributions were separated by 1.70 (1.18) *D* units, and the adapting distribution was skewed toward negative values (skewness of −0.24), whereas the buildup *D* values were skewed toward positive values (skewness of +1.16). Also shown are the responses with the same number of spikes in the C_i and C_f intervals (black histogram; $n = 31$) and those with no spiking response in either the initial or final portion of the conditioner (green histogram; $n = 129$). Both of these conditioner response types were associated with enhancement (see figure legend for distribution statistics).

Enhancement was not clearly related to the presence of a postinhibitory rebound spiking response after the conditioner. The example conditioner-alone responses shown above Figure 5*A* are typical in that they show no indication of offset-locked rebound or persistence. In fact, the majority of responses immediately after the conditioner alone were driven below spontaneous rate (530 of 905 observations). Among the 316 instances of enhancement ($D > 1$), 189 (60%) were generated by conditioners that caused a drop in spiking after their offset (supplemental Fig. S2, available at www.jneurosci.org as supplemental material). Any enhancement of the test-complex response must have overcome this simultaneously present forward suppression in these neurons.

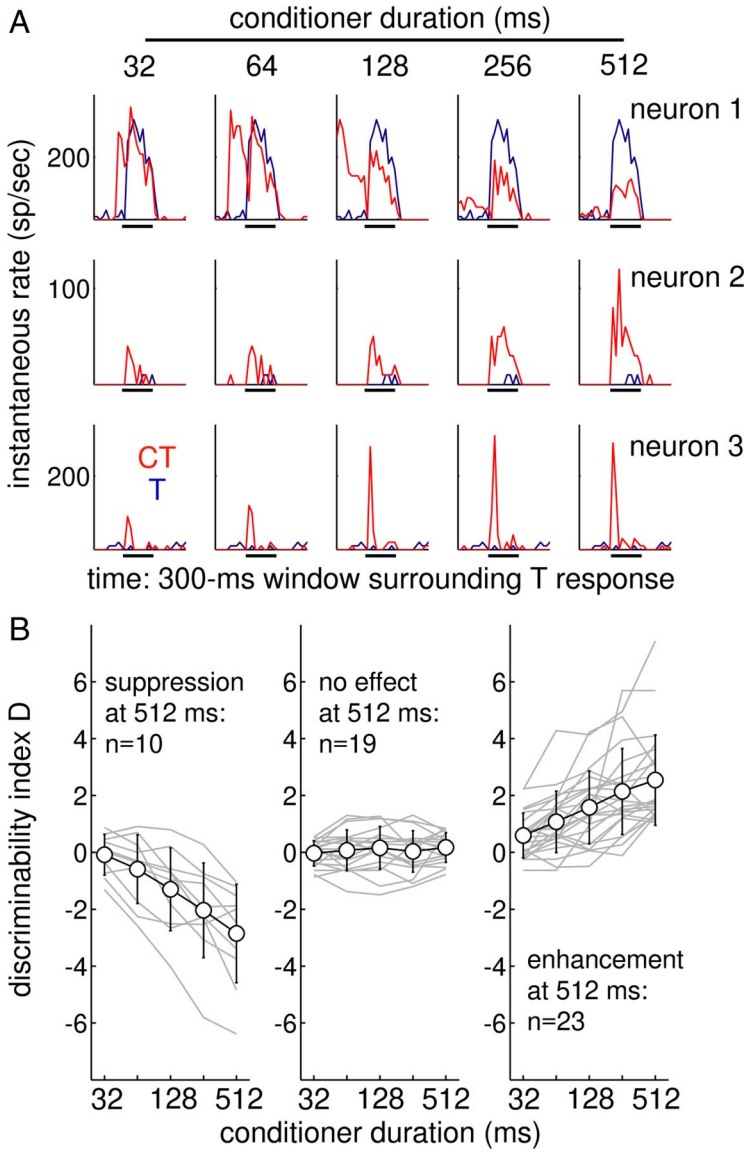

Figure 4. The strength of enhancement and suppression increases as the conditioner duration is lengthened. ***A***, Short-time-window CT (red) and T (blue) responses of three neurons tested over a range of conditioner durations. Bars under the panels show the position of the T response window. ***B***, Dependence of the *D* statistic on conditioner duration in a larger group of neurons, separated according to the *D* value with a 512 ms conditioner. Criteria are $D < -1$ for suppression and $D > 1$ for enhancement. Functions for individual cells are shown in gray; across-neuron averages ± SD are drawn with black circles. The average suppression function (left) crosses $D = -2$ at 247 ms; the enhancement average (right) first exceeds $D = +2$ with a 215ms conditioner.

Neural detection thresholds

One of the most straightforward ways to measure enhancement in psychophysics is to vary the level of the "probe" component within the context of the simultaneous flanking bands of the test complex until it is just detectable. Enhancement can then be defined as the decibel difference in thresholds with and without the preceding conditioner. The data presented so far cannot directly address the question of the magnitude of the detection-threshold shift in IC neurons, because the probe component was always fixed at an SPL equal to that of all of the other components in the test and conditioner. To address this issue, we varied the level of the BF component (with and without the conditioner) over a 30 dB range in 41 CNIC neurons while holding the other component SPLs fixed. Some cells were tested with two or three overall SPLs; the BF probe level was varied with respect to the level of the other components in the stimulus.

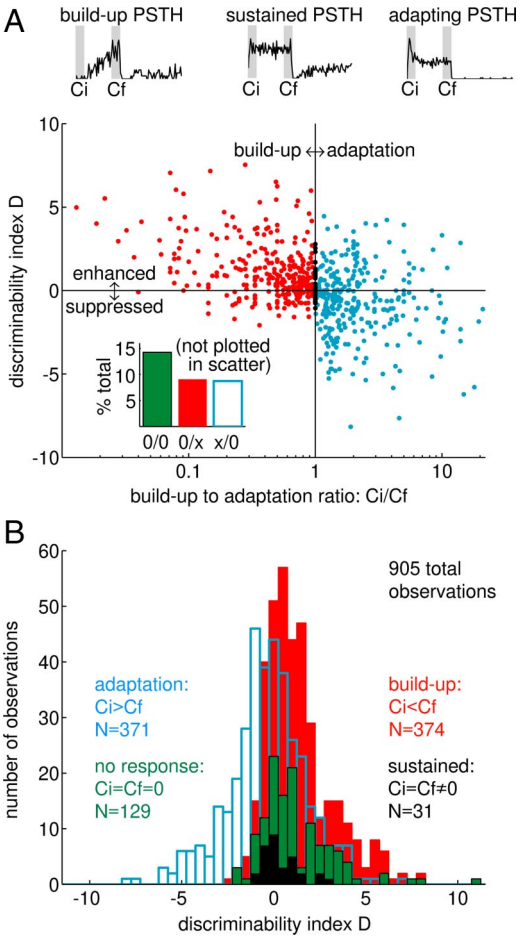

Figure 5. Buildup conditioner responses are associated with enhancement of the subsequent test stimulus response. ***A***, Test-response discriminability as a function of the ratio between the firing rates during the initial and final 100 ms of the conditioner response (C_i/C_f). Example PSTHs are shown above the panel for three conditioner responses spanning a range of buildup to adaptation ratio values. Data from 101 neurons tested using five conditioner NWs are shown; some neurons are represented more than once if different SPLs were tested, resulting in 905 total comparisons (i.e., on average, ~9 stimulus conditions were tested per neuron). Inset, Proportions of responses that are not included in the main panel as a consequence of an observation of zero spikes in one or both of the 100 ms counting windows. ***B***, Distributions of the *D* index for four conditioner response types, as defined in the panel (all 905 *D* value comparisons are included in ***B***). Mean, median, and skewness of four distributions: adaptation, −0.37, −0.31, −0.24; buildup, 1.33, 0.87, 1.16; no response, 0.75, 1.16, 1.82; sustained, 0.38, 0.18, 0.89.

Responses in the form of PSTHs for two neurons to the 30 dB range of BF probe levels are shown in Figure 6, *A* and *B*. Darker lines represent higher SPL probe components. To objectively define a neural detection threshold in the two conditions, the mean and variability of the 10 repetitions of each stimulus were analyzed. These quantities are plotted in Figure 6, *A2* and *B2*. The leftmost point in these panels represents the "comparison" firing rate measured when the BF component was absent (labeled CA for "conditioner alone" along the *x*-axis). In neuron 1, the comparison rates were both zero in the T and CT conditions. In neuron 2, however, the comparison rates were different, with the T comparison rate higher than that of the CT response. This difference reflects the adapting profile of the response to the conditioner (Fig. 6*B3*) and has an important influence on the next (and final) step in the process of determining thresholds. We used the *D* statistic to identify the lowest BF probe level that elicited a rate significantly different from the comparison (CA) rate. Threshold was defined as the lowest level that resulted in a *D* value of one or greater. *D* functions for the two examples are shown in Figure 6, *A4* and *B4*. The analysis reveals that threshold levels were lower with the conditioner (CT) than without it (T) in both neurons (vertical dashed lines are positioned at the abscissa values corresponding to threshold in the two stimulus configurations). Note that the difference in comparison (CA) firing rate distributions, along with different inflection points in the *D* functions, contribute to the threshold shift in neuron 2.

Across the sample, the sign of the threshold shift was strongly biased toward negative values, indicating lower thresholds for the BF probe when the conditioner was present than when it was not (Fig. 6*C*,*D*). The magnitude of the threshold shift depended on the overall level of the flanking components (Fig. 6*C*) in a way broadly consistent with the enhancement measured using equal-SPL probe and conditioner/test-complex components (Fig. 2). The 40 dB SL condition yielded the most consistent trend toward enhancement, with a median threshold shift of 14.6 dB, although it should be pointed out that the stimuli used here all had NWs of 0.5 octaves, which appeared to be nearly optimal for generating enhancement with the 40 dB SL stimulus (Fig. 2). The spread of near-BF excitation at high levels likely led to more within-channel forward suppression of the test complex and a wider spread of threshold shifts across neurons in the 60 dB SL condition.

One of the initial motivations for measuring neural detection thresholds was to confirm the relevance of our suprathreshold *D* measurements (Figs. 1–5) for comparisons with psychophysical measures of enhancement. To determine this relationship, the same threshold shifts shown in Figure 6*C* are plotted as a function of the *D* statistic (as measured with an equal-amplitude BF component) in Figure 6*D*. The two metrics are significantly correlated with one another ($r = -0.395$, $p = 0.0026$, excluding the outlier at $D = -6$): positive values of suprathreshold *D* (reflecting enhancement) were predictive of negative threshold shifts (i.e., in the direction of enhancement). Clearly, the relationship does not allow for a particularly precise prediction of a threshold shift given a specific *D* value, but the general trend for a bias toward enhanced responses is present both near and above detection threshold for the BF probe.

Phenomenological model

A model of auditory processing was simulated to test whether simple interactions between broadly tuned inhibition and more sharply tuned excitation could account for the major features of the data (for details, see Materials and Methods). Ideally, a parsimonious model would be able to predict (1) both enhancement and suppression of the test stimulus (Figs. 1, 2), (2) a nonmonotonic dependence of *D* on the stimulus NW (Fig. 2*B*,*C*), (3) a stronger dependence on the low-frequency conditioner components in the generation of test-response modulation (Fig. 3*B*), and (4) increased enhancement or suppression with increasing conditioner duration (Fig. 4).

Example intermediate model responses (smoothed versions of the excitation and delayed inhibition) are shown in Figure 7*A* for a T stimulus and in Figure 7*B* for a CT stimulus (NW = 0.7 octaves, 60 dB SL). Three different overall strengths of inhibition (S_{inh}) are drawn in each panel (black, orange, and green curves). The excitatory responses (blue) are essentially the output of a single model AN fiber with a BF equal to the probe frequency of 4 kHz. Note that the test-response excitation is reduced given the presentation of the conditioner (compare blue responses in Fig. 7*A*,*B*); in the model, this is a result of simple firing-rate adapta-

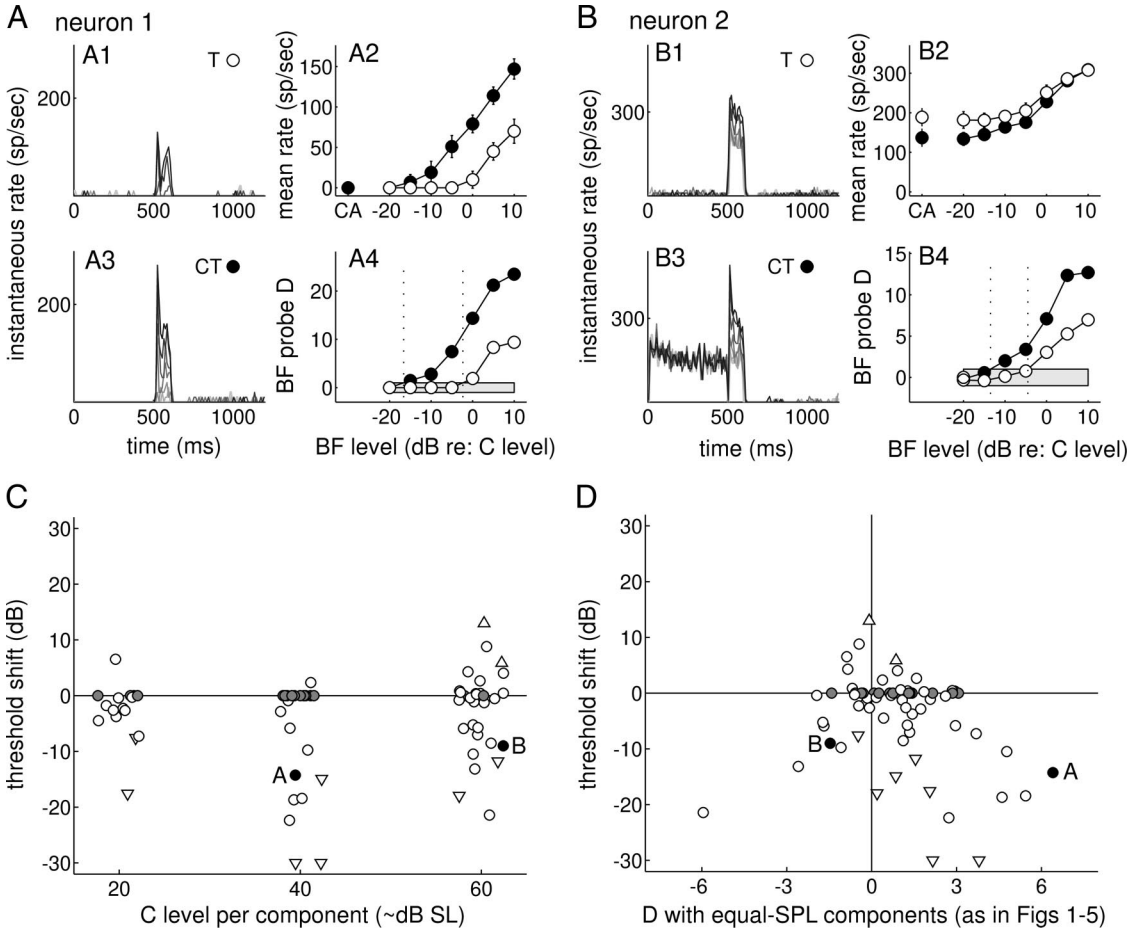

Figure 6. Neural detection thresholds for the BF tone are usually lower in the presence of a preceding conditioner. ***A***, ***B***, Responses from two example neurons to stimuli using a 30 dB range of probe SPLs. ***A1***, ***B1***, Test-alone response PSTHs (darker lines correspond to higher-SPL BF tones); ***A2***, ***B2***, Average rates from the 100 ms test-response window. Open circles, Test alone; filled circles, conditioner-then-test stimulus. CA refers to conditioner-alone rate responses generated from the initial (open circles) and final (filled circles) 100 ms response to the conditioner. ***A3***, ***B3***, PSTHs for the conditioner followed by the test stimulus over the same range of BF tone levels; ***A4***, ***B4***, Quantification of the differences between the rate responses in ***A2*** and ***B2*** (divided by the across-repetition rate estimate SD) in the CA case to the conditions with a BF tone present. Gray boxes highlight the range of BF levels that resulted in $|D| < 1$. Vertical dashed lines are placed at the threshold BF level (i.e., the lowest level resulting in $D > 1$). ***C***, Threshold shifts across the sample between the T and CT conditions. Negative values indicate an enhanced (lower) detection threshold in the CT case. Some neurons were tested at multiple overall levels; they are included up to three times in the panel. ***D***, Threshold shift for the same set of responses as a function of the *D* statistic (CT vs T) measured using an equal-amplitude BF tone (as in Figs. 1–5). The two neurons illustrated in ***A*** and ***B*** are plotted with filled black symbols and are labeled in ***C*** and ***D***. Filled gray circles indicate neurons whose thresholds were below the lowest SPL tested in both the CT and T conditions (arbitrarily plotted at a 0 dB threshold shift). Downward (upward) triangles represent cases in which the T (CT) threshold was higher than the highest level tested and was thus set to that highest level (+10 dB for C level).

tion of excitation caused by the conditioner and is consistent with real AN recordings (Palmer et al., 1995). In response to the conditioner, the inhibitory inputs tend to adapt much more strongly over time than the excitation (Fig. 7*B*) because their broader frequency tuning allows for a stronger contribution of off-BF components to the overall response.

When the inhibition was subtracted from the excitation, the interplay between their temporal response profiles resulted in the final model responses shown in Figure 7, *C* and *D*, again for the T and CT stimulus configurations. The difference signal CT − T is shown in Figure 7*E*. When the inhibition was silenced ($S_{inh} = 0$), the model predicts a suppressive effect of the conditioner (black curves), but when the relative strength is chosen appropriately, the model can exhibit robust enhancement (orange curves). Interestingly, the model conditioner responses buildup in this case, consistent with the analyses described in Figure 5 of the real IC data. For stronger inhibition, responses to the test stimulus were limited to its onset, and the modulation of the overall response caused by the conditioner became negligible (green curves). The test-response difference signals (i.e., 500–600 ms in Fig. 7*E*) clearly show both enhancement (orange) and suppression (black), depending on the chosen value of the inhibitory strength of the model. The duration of the T response enhancement or suppression (~100 ms) (Fig. 7*E*) is a direct reflection of the adaptation time constants included in the AN model (Heinz et al., 2001).

To allow *D* to be computed, noise was added to the test–stimulus rates with an amplitude based on the across-repetition rate SD observed in the actual data (supplemental Fig. S3, available at www.jneurosci.org as supplemental material). Test-complex average rate differences (CT − T) were normalized by this assumed SD to compute *D*. The model *D* values depended heavily on both the strength of inhibition and the NW (Fig. 7*F*). As suggested by the examples in Figure 7*A–E*, test responses were suppressed regardless of NW if the inhibitory input was too weak (<0.05). Only within a circumscribed region of S_{inh} and NW was enhancement observed; a cross-section of the contour plot in Figure 7*F* at an S_{inh} value of 0.1 results in a non-monotonic *D* versus NW function, with suppression at very narrow NWs, enhancement within a range from ~0.5 to 1.5 octaves, and no effect

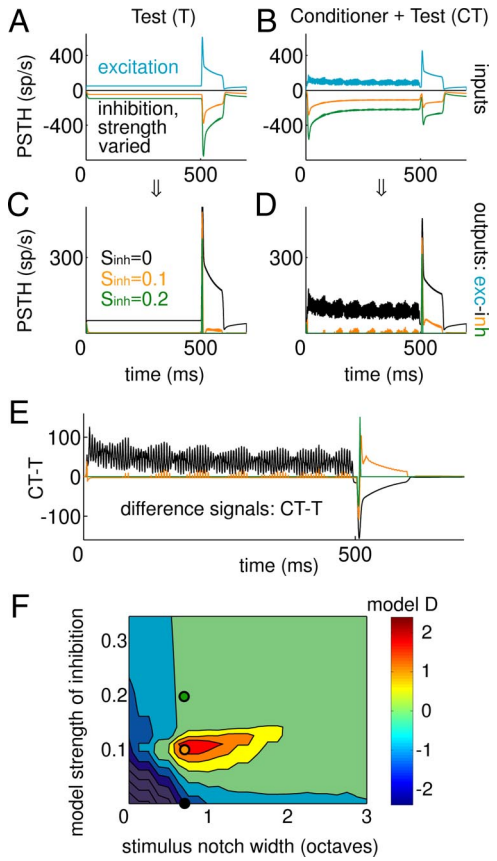

Figure 7. A phenomenological model with adapting inhibition that is more broadly tuned than excitation predicts both enhancement and suppression. Intermediate model responses are shown in ***A*** for a test-alone stimulus and in ***B*** for a conditioner-then-test case (stimulus NW = 0.7 octaves, 60 dB SL). Excitatory responses (blue) were fixed in the model; the hypothetical inhibitory inputs (plotted with negative values in ***A*** and ***B***) were varied in strength (this parameter is labeled S_{inh}). ***C***, Corresponding model outputs for the test stimulus using the inputs shown in ***A*** and ***B*** (excitation − inhibition, rectified). ***D***, Same for the conditioner-then-test stimulus. ***E***, Difference signal plots for the three strengths of inhibition illustrated in ***A–D*** (compare with those in Fig. 2). ***F***, Regions of enhancement and suppression in the model over a range of inhibitory strengths and stimulus notch widths. Filled circles correspond to the three inhibitory strengths for the models in ***C–E***.

of the conditioner beyond a 2 octave NW (compare Fig. 2*B*,*C*). For stronger inhibitory strengths, suppression was still present at small NWs, but enhancement did not emerge at larger NWs.

The model also recapitulates other salient features of the data (supplemental Fig. S4, available at www.jneurosci.org as supplemental material), including the saturating but robust level dependence, stronger reliance on the low-frequency conditioner components to generate enhancement, and the buildup of the phenomenon with increasing conditioner duration (although the model does not predict any increase in conditioner effects beyond a duration of ~128 ms). Supplemental Figure S4 (available at www.jneurosci.org as supplemental material) also includes predicted *D* values for several other versions of the model with different frequency tuning properties of the inhibitory input channel. These parameters are crucial for reasonable predictions of the NW dependence of the effect: inhibition with effectively broader tuning than that assumed in Figure 7 leads to enhancement that can persist for stimuli with NWs >2 octaves, a feature rarely encountered in our data. If the inhibitory tuning is set equal to that of the excitation, no choice of overall inhibitory strength results in enhanced test responses. Therefore, the strength and frequency tuning patterns of the inhibitory input in the model are both critical features that can be constrained in a straightforward way by the data.

Discussion

Conditioner-induced enhancement and suppression of test-complex responses were both observed in CNIC neurons. Variations in several stimulus parameters all revealed qualitative similarities between CNIC responses and perceptual measures of enhancement (Carlyon et al., 1989; Viemeister, 1980; Wright et al., 1993). A phenomenological model with time-varying inhibitory and excitatory inputs that had a common BF but more broadly tuned inhibition was able to predict many salient features of the data (Viemeister and Bacon, 1982).

Inherited or emergent?

Extracellular recordings do not allow us to directly comment on the question of whether enhancement is established at lower levels of the system and passed along or generated at the level of the colliculus. We can, however, make some inferences based on previous studies. For example, single AN fibers do not exhibit enhanced test-complex responses (Palmer et al., 1995). Therefore, the effect is most likely a consequence of across-frequency processing in the CNS. Some neurons in the ventral cochlear nucleus (the first stage of central auditory processing) do appear to show a relatively small amount of response enhancement (Scutt, 2000) during the initial 10 or 20 ms of the test response. It may be fruitful to study responses to enhancement stimuli in neurons of the inhibition-rich dorsal cochlear nucleus, in which stimuli as simple as two tones have revealed robust context-dependent facilitation, especially in neurons with buildup response patterns (Boettcher et al., 1990; Palombi et al., 1994). Overall, it seems likely that enhancement is generated gradually and accumulates along the auditory pathway as a consequence of the hardwired convergence of inhibitory and excitatory inputs. The prolonged duration of the effect we observed in IC neurons (≥100 ms) (Fig. 2*B*) is probably mediated by higher-level interactions and is more likely to be an emergent property than the initial test-response facilitation (which could be inherited from lower levels).

Possible mechanisms of enhancement

The model we used to account for enhancement and suppression is phenomenological in nature and does not rely on an explicit set of mechanisms (beyond generic interactions between inhibition and excitation). The fact that responses to the conditioner alone did not typically include an excitatory offset or persistent response (supplemental Fig. S2, available at www.jneurosci.org as supplemental material) suggests that neither postinhibitory rebound (Sivaramakrishnan and Oliver, 2001) nor reverberant long-lasting excitation resulting from reciprocal excitatory connections (McCormick et al., 2003) are required to elicit enhancement in CNIC neurons.

The anatomical presence (Winer, 2005) and functional impact (Suga and Ma, 2003) of corticofugal connections leave open the possibility that descending (efferent) projections could also give rise to the context-dependent responses observed in the IC. Focal electrical stimulation of bat cortex results in enhanced responses near the stimulated BF in subcortical structures (including IC), but this takes several minutes to develop (Luo et al., 2008). It is not clear whether actual sound stimulation could activate this modulatory system quickly enough to account for the time course of response facilitation we observe in IC (on the order of tens or hundreds of milliseconds) (Fig. 4).

The olivocochlear (OC) efferent system has also been implicated as a potential source for the generation of enhanced detectability of delayed-onset tonal signals presented in a notched-noise background (Strickland, 2004). This hypothesis predicts that enhancement should be reflected directly in the responses of AN fibers; for the stimuli used in the current study, this is not the case, at least in anesthetized guinea pigs (Palmer et al., 1995). It remains possible that the anesthetic regimen used in the AN study could have reduced the impact of this feedback pathway, but it seems unlikely that the entire effect is caused by an anesthetic-sensitive component of the OC system, especially because clear effects of OC system manipulation have been shown in other experiments using anesthetized animals (Kawase et al., 1993).

Insights from the model

The convergence of inhibition and excitation in the IC is well documented (Oliver, 2004; Davis, 2005), and several functional consequences in pure-tone and broadband stimulus responses have been identified (Faingold et al., 1989; Palombi and Caspary, 1996; LeBeau et al., 2001; Davis, 2002; Davis et al., 2003; May et al., 2008). Here we have shown that the variation of a single parameter in a model, the relative strength of inhibition, provides a straightforward explanation for the heterogeneity of responses observed across neurons in the pop-out paradigm. A circumscribed region of inhibitory strength and stimulus notch width resulted in enhancement; outside of these parameters, the model predicted either suppression or negligible effects of the conditioner on the test responses (Fig. 7). Although this is a simplification of the real situation, it does reinforce the idea that the interplay between time-varying inhibition and excitation can potentially explain many nonlinear phenomena in the responses of CNIC neurons (Casseday et al., 1994; Sinex et al., 2005; Nelson and Carney, 2007; Leary et al., 2008).

If the decline in the effective strength of inhibition over time in IC neurons were determined entirely by the adaptation profile of its inputs, then one might expect to see very slowly adapting responses in its known sources of inhibitory input (to account for the gradual buildup effects shown in Fig. 4). At first glance, this does not appear to be the case [e.g., dorsal nucleus of the lateral lemniscus (Kuwada et al., 2006), ventral nucleus of the lateral lemniscus (Batra and Fitzpatrick, 2002), and lateral superior olive (Moore and Caspary, 1983)]. At least three different explanations could account for this: (1) the buildup of enhancement (or suppression) is an emergent property of the IC; (2) adaptation in subcollicular inhibitory input structures is different for BF tones than for broadband and/or off-BF sounds; or (3) long-term adaptation in the input structures is not apparent in previous studies because the stimuli were not sufficiently long to observe such slow decay. This final possibility is an often overlooked but potentially important aspect of auditory responses, with long-term power-law type adaptive behavior emerging as early in the pathway as the auditory nerve (Kiang et al., 1965; Zilany et al., 2009) and persisting in responses of various brainstem nuclei when tested with sufficiently long stimuli to observe such effects (Goldberg et al., 1964; Goldberg and Greenwood, 1966; Tsuchitani and Boudreau, 1966).

Another feature of the model that is required to predict enhancement is the relatively broad bandwidth of inhibition with respect to excitation. This is a departure from a previous version of a similar model that used identical tuning profiles for inhibition and excitation to predict responses to narrow-band temporally fluctuating sounds (Nelson and Carney, 2004). When this implementation of the model was tested, only suppression was observed (supplemental Fig. S4, available at www.jneurosci.org as supplemental material). It is possible that the two different assumed patterns of overlap could both exist across the population and that this difference underlies the presence of enhancement or suppression. There is some evidence for the existence of two such groups, with approximately similar rates of occurrence (Palombi and Caspary, 1996).

Psychophysically, enhancement is readily elicited with either monaural (Carlyon et al., 1989) or diotic (identical in the two ears) stimulation (Serman et al., 2008) but not when the conditioner and test stimuli are delivered to opposite ears (Viemeister, 1980; Summerfield et al., 1987; Carlyon et al., 1989; Kidd and Wright, 1994). All of the data presented here represent responses to free-field (and thus approximately diotic) sound stimulation. Previous work has shown that activation of the ipsilateral ear often results in an inhibitory net effect (Kuwada et al., 1997; Davis et al., 1999; Bauer et al., 2000) that gets weaker over time (Zhang and Kelly, 2009), consistent with the adaptation-of-inhibition hypothesis. Additional examination of this issue using closed-field, binaural sound stimulation that can be adjusted independently in the two ears might resolve some of the uncertainty regarding the specific pathways that are required to generate enhancement and suppression in the IC.

Age-related hearing loss leads to compensatory changes in the CNS, including a downregulation of GABAergic inhibition (Caspary et al., 2008). If, as assumed in the model, such inhibitory processes are required to generate enhancement, it follows that listeners with hearing impairment should exhibit less of an effect. This is indeed the case, at least for forward masking and speech-formant enhancement paradigms (Thibodeau, 1991). To our knowledge, shifts in probe signal detection thresholds have not been measured in hearing-impaired listeners. It is possible that the relatively high across-subject variability observed even in normal-hearing listeners in enhancement tasks (Wright et al., 1993) could reflect differences in central inhibitory processing that are not revealed by pure-tone threshold evaluations of hearing acuity.

Conclusions

Our data reflect a fundamental transformation in the nature of the neural code for stimuli that pop out perceptually between the auditory nerve and the inferior colliculus. A distributed, relative representation of enhanced sounds in the periphery provides the input to early central processing stages, resulting in explicit response facilitation in single neurons by the level of the midbrain. Adapting inhibitory influences provide a parsimonious explanation for the neural phenomenon, and realistic assumptions for excitatory and inhibitory interactions within a phenomenological model allow for reasonable predictions of many features of the observed responses.

References

Batra R, Fitzpatrick DC (2002) Processing of interaural temporal disparities in the medial division of the ventral nucleus of the lateral lemniscus. J Neurophysiol 88:666–675.

Bauer EE, Klug A, Pollak GD (2000) Features of contralaterally evoked inhibition in the inferior colliculus. Hear Res 141:80–96.

Boettcher FA, Salvi RJ, Saunders SS (1990) Recovery from short-term adaptation in single neurons in the cochlear nucleus. Hear Res 48:125–144.

Carlyon RP, Buus S, Florentine M (1989) Changes in the masked thresholds of brief tones produced by prior bursts of noise. Hear Res 42:37–45.

Caspary DM, Ling L, Turner JG, Hughes LF (2008) Inhibitory neurotransmission, plasticity and aging in the mammalian central auditory system. J Exp Biol 211:1781–1791.

Casseday JH, Ehrlich D, Covey E (1994) Neural tuning for sound duration:

role of inhibitory mechanisms in the inferior colliculus. Science 264: 847–850.
Davis KA (2002) Evidence of a functionally segregated pathway from dorsal cochlear nucleus to inferior colliculus. J Neurophysiol 87:1824–1835.
Davis KA (2005) Spectral processing in the inferior colliculus. Int Rev Neurobiol 70:169–205.
Davis KA, Ramachandran R, May BJ (1999) Single-unit responses in the inferior colliculus of decerebrate cats. II. Sensitivity to interaural level differences. J Neurophysiol 82:164–175.
Davis KA, Ramachandran R, May BJ (2003) Auditory processing of spectral cues for sound localization in the inferior colliculus. J Assoc Res Otolaryngol 4:148–163.
Faingold CL, Gehlbach G, Caspary DM (1989) On the role of GABA as an inhibitory neurotransmitter in inferior colliculus neurons: iontophoretic studies. Brain Res 500:302–312.
Goldberg JM, Greenwood DD (1966) Response of neurons of the dorsal and posteroventral cochlear nuclei of the cat to acoustic stimuli of long duration. J Neurophysiol 29:72–93.
Goldberg JM, Adrian HO, Smith FD (1964) Response of neurons of the superior olivary complex of the cat to acoustic stimuli of long duration. J Neurophysiol 27:706–749.
Green DM, Swets JA (1966) Signal detection theory and psychophysics. New York: Wiley.
Hall JW, Haggard MP, Fernandes MA (1984) Detection in noise by spectro-temporal pattern analysis. J Acoust Soc Am 76:50–56.
Hartmann WM, Goupell MJ (2006) Enhancing and unmasking the harmonics of a complex tone. J Acoust Soc Am 120:2142–2157.
Heinz MG, Zhang X, Bruce IC, Carney LH (2001) Auditory nerve model for predicting performance limits of normal and impaired listeners. Acoust Res Lett Online 2:91–96.
Jesteadt W, Bacon SP, Lehman JR (1982) Forward masking as a function of frequency, masker level, and signal delay. J Acoust Soc Am 71:950–962.
Kawase T, Delgutte B, Liberman MC (1993) Antimasking effects of the olivocochlear reflex. II. Enhancement of auditory-nerve response to masked tones. J Neurophysiol 70:2533–2549.
Kiang NYS, Watanabe T, Thomas EC, Clark LF (1965) Discharge patterns of single fibers in the cat's auditory nerve, MIT Research Monograph 35. Cambridge, MA: Massachusetts Institute of Technology.
Kidd G Jr, Wright BA (1994) Improving the detectability of a brief tone in noise using forward and backward masker fringes: monotic and dichotic presentations. J Acoust Soc Am 95:962–967.
Kuwada S, Batra R, Yin TC, Oliver DL, Haberly LB, Stanford TR (1997) Intracellular recordings in response to monaural and binaural stimulation of neurons in the inferior colliculus of the cat. J Neurosci 17:7565–7581.
Kuwada S, Fitzpatrick DC, Batra R, Ostapoff EM (2006) Sensitivity to interaural time differences in the dorsal nucleus of the lateral lemniscus of the unanesthetized rabbit: comparison with other structures. J Neurophysiol 95:1309–1322.
Leary CJ, Edwards CJ, Rose GJ (2008) Midbrain auditory neurons integrate excitation and inhibition to generate duration selectivity: an *in vivo* whole-cell patch study in anurans. J Neurosci 28:5481–5493.
LeBeau FE, Malmierca MS, Rees A (2001) Iontophoresis *in vivo* demonstrates a key role for $GABA_A$ and glycinergic inhibition in shaping frequency response areas in the inferior colliculus of guinea pig. J Neurosci 21:7303–7312.
Lu T, Liang L, Wang X (2001) Neural representations of temporally asymmetric stimuli in the auditory cortex of awake primates. J Neurophysiol 85:2364–2380.
Luo F, Wang Q, Kashani A, Yan J (2008) Corticofugal modulation of initial sound processing in the brain. J Neurosci 28:11615–11621.
May BJ, Anderson M, Roos M (2008) The role of broadband inhibition in the rate representation of spectral cues for sound localization in the inferior colliculus. Hear Res 238:77–93.
McCormick DA, Shu Y, Hasenstaub A, Sanchez-Vives M, Badoual M, Bal T (2003) Persistent cortical activity: mechanisms of generation and effects on neuronal excitability. Cereb Cortex 13:1219–1231.
Moore MJ, Caspary DM (1983) Strychnine blocks binaural inhibition in lateral superior olivary neurons. J Neurosci 3:237–242.
Nelson PC, Carney LH (2004) A phenomenological model of peripheral and central responses to amplitude-modulated tones. J Acoust Soc Am 116:2173–2186.
Nelson PC, Carney LH (2007) Neural rate and timing cues for detection and discrimination of amplitude-modulated tones in the awake rabbit inferior colliculus. J Neurophysiol 97:522–539.
Nelson PC, Smith ZM, Young ED (2009) Wide-dynamic-range forward suppression in marmoset inferior colliculus neurons is generated centrally and accounts for perceptual masking. J Neurosci 29:2553–2562.
Oliver DL (2004) Neuronal organization in the inferior colliculus. In: The inferior colliculus (Winer JA, Schreiner CA, eds), pp 69–114. New York: Springer.
Palmer AR, Summerfield Q, Fantini DA (1995) Responses of auditory-nerve fibers to stimuli producing psychophysical enhancement. J Acoust Soc Am 97:1786–1799.
Palombi PS, Caspary DM (1996) GABA inputs control discharge rate primarily within frequency receptive fields of inferior colliculus neurons. J Neurophysiol 75:2211–2219.
Palombi PS, Backoff PM, Caspary DM (1994) Paired tone facilitation in dorsal cochlear nucleus neurons: a short-term potentiation model testable in vivo. Hear Res 75:175–183.
Ramachandran R, Davis KA, May BJ (1999) Single-unit responses in the inferior colliculus of decerebrate cats. I. Classification based on frequency response maps. J Neurophysiol 82:152–163.
Relkin EM, Turner CW (1988) A reexamination of forward masking in the auditory nerve. J Acoust Soc Am 84:584–591.
Scutt MJ (2000) Temporal enhancement in the cochlear nucleus of the guinea pig. PhD thesis, University of Nottingham.
Serman M, Semal C, Demany L (2008) Enhancement, adaptation, and the binaural system. J Acoust Soc Am 123:4412–4420.
Simpson AJ, Fitter MJ (1973) What is the best index of detectability? Psychol Bull 80:481–488.
Sinex DG, Li H, Velenovsky DS (2005) Prevalence of stereotypical responses to mistuned complex tones in the inferior colliculus. J Neurophysiol 94:3523–3537.
Sivaramakrishnan S, Oliver DL (2001) Distinct K currents result in physiologically distinct cell types in the inferior colliculus of the rat. J Neurosci 21:2861–2877.
Strickland EA (2004) The temporal effect with notched-noise maskers: analysis in terms of input-output functions. J Acoust Soc Am 115:2234–2245.
Suga N, Ma X (2003) Multiparametric corticofugal modulation and plasticity in the auditory system. Nat Rev Neurosci 4:783–794.
Summerfield Q, Sidwell A, Nelson T (1987) Auditory enhancement of changes in spectral amplitude. J Acoust Soc Am 81:700–708.
Thibodeau LM (1991) Performance of hearing-impaired persons on auditory enhancement tasks. J Acoust Soc Am 89:2843–2850.
Tsuchitani C, Boudreau JC (1966) Single unit analysis of cat superior olive S segment with tonal stimuli. J Neurophysiol 29:684–697.
Viemeister NF (1980) Adaptation of masking. In: Psychophysical, physiological, and behavioral studies in hearing (van den Brink G, Bilsen FA, eds), pp 190–199. Delft, The Netherlands: Delft UP.
Viemeister NF, Bacon SP (1982) Forward masking by enhanced components in harmonic complexes. J Acoust Soc Am 71:1502–1507.
Winer JA (2005) Decoding the auditory corticofugal systems. Hear Res 207:1–9.
Wright BA, McFadden D, Champlin CA (1993) Adaptation of suppression as an explanation of enhancement effects. J Acoust Soc Am 94:72–82.
Yost WA, Sheft S (1989) Across-critical-band processing of amplitude-modulated tones. J Acoust Soc Am 85:848–857.
Zhang H, Kelly JB (2009) Time-dependent effects of ipsilateral stimulation on contralaterally evoked responses in the rat's central nucleus of the inferior colliculus. Brain Res 1303:48–60.
Zilany MS, Bruce IC, Nelson PC, Carney LH (2009) A phenomenological model of the synapse between the inner hair cell and auditory nerve: long-term adaptation with power-law dynamics. J Acoust Soc Am 126: 2390–2412.